1988

Remote Near-IR Reflectance Measurements with the Use of a Pair of Optical Fibers and a Fourier Transform Spectrometer

D. D. Archibald

Charles E. Miller
Haverford College

L. T. Lin

D. E. Honigs

Remote Near-IR Reflectance Measurements with the Use of a Pair of Optical Fibers and a Fourier Transform Spectrometer

D. D. ARCHIBALD, C. E. MILLER, L. T. LIN, and D. E. HONIGS*
Department of Chemistry, University of Washington, Seattle, Washington 98195

A commercial near-infrared (near-IR) Fourier transform (FT) spectrometer was modified to make remote reflectance measurements over a single optical fiber or pair of optical fibers. With the use of two low-hydroxyl fused-silica optical fibers and an InSb detector, the near-IR region from 0.92 to 2.15 μm was measurable. An InGaAs detector was used to obtain reflectance spectra over the region from 0.92 to 1.56 μm. With this detector, single-fiber reflectance and transmission measurements were possible and a variety of dual-fiber probe geometries could be easily employed. Dual-fiber geometries were used to enhance pathlength, to perform depth discrimination, and to make measurements without physical contact between the probe and the specimen. Potential applications and improvements are discussed.

Index Headings: **Spectroscopy (near-IR, reflectance, remote, FT-IR); Optical fiber; Depth discrimination; Spatial resolution.**

INTRODUCTION

Near-IR reflectance analysis is a powerful technique for quantitative analysis of complex mixtures including textiles, papers, and agricultural, pharmaceutical, or industrial powders. Several very good reviews address both the fundamental and application aspects of near-IR spectroscopy.[1,2,3] The success of near-IR reflectance analysis is a result of several attributes of near-IR spectroscopy. Near-IR light penetrates deeply into the specimen and the generally low near-IR absorptivities result in linear calibrations. The deep penetration of near-IR light into a specimen often allows analysis of the specimen with little or no sample preparation. Moreover, near-IR analysis can detect subtle differences between specimens because C-H, N-H, and O-H combination and overtone absorption bands are very sensitive to their chemical and physical environment. Equally important, excellent S/N can be obtained with near-IR instrumentation, and mathematical algorithms are available to perform calibrations for complex mixtures.

As noted above, near-IR analysis is highly amenable to quantitative analysis of solid specimens in a relatively unperturbed state. However, in most cases, the specimen must still be brought to the spectrometer, and this requirement might be inconvenient, time-consuming, or costly, and might result in the destruction or alteration of the specimen. The ability to easily and efficiently perform near-IR reflectance analysis on the specimen in its original location would greatly increase the applicability of this technique, particularly in the areas of process chemistry and medical monitoring. Optical fibers are a nearly ideal means to accomplish remote near-IR analysis because they transmit near-IR light with low loss over long distances and they are flexible. Fiber-optic reflectance probes have been incorporated into commercial dispersive near-IR spectrometers, but these normally consist of fiber bundles that are expensive for long distance measurements. Not only are fiber bundles expensive, but the large size and inflexibility of fiber bundles also can prevent use of a fiber bundle probe on small specimens or specimens with limited access.

The suitability of an FT-IR spectrometer to remote spectroscopy performed over a single optical fiber was described in an earlier paper.[4] It has been reported that an FT spectrometer is suitable for measurement of near-IR light transmitted through a single optical fiber,[5,6] and this application was shown to be useful for remote near-IR transmission measurements.[4] We have extended these results to the realm of reflectance spectroscopy by employing better transmitting optical fibers and more sensitive detection.

EXPERIMENTAL

A modified Perkin-Elmer FT-IR 1800 with a near-IR attachment was used for all the measurements. The detection system consisted of a liquid-nitrogen-cooled InSb ($D^* = 2.5 * 10^{11}$ cm * $Hz^{1/2}$ * W^{-1}) or, alternatively a nitrogen-cooled InGaAs detector ($D^* = 4.4 * 10^{12}$ cm * $Hz^{1/2}$ * W^{-1}). Both detectors had 1-mm-diameter active areas. The InSb detector (IR Associates) was suitable for the near-IR region from 0.92 to 2.86 μm when used in conjunction with the SiO_2 beamsplitter and the standard detector optic in the FT-IR. With the InGaAs detector (Electro-Optical Systems), the spectral region was limited to 0.92–1.56 μm, and the detector optics were modified in a manner similar to that described in the earlier report.[4] Triangular apodization was used on each interferogram, and the spectra were calculated as the magnitude of the Fourier transform. Nominal resolution was 8 cm^{-1} for most of the spectra. With the InGaAs detector, single scans at 8-cm^{-1} nominal resolution lasted from 0.27 to 2.7 s, depending on the mirror velocity that was selected. Spectra were signal averaged for up to 4.5 min.

For each measurement, the source optic collected light emanating from the end of a 600-μm core diameter, 0.25 numerical aperture (NA), low-hydroxyl fused-silica glass-clad optical fiber (Fiberguide Industries). The single-fiber reflectance probe consisted of a 6-m length of optical fiber with a back-illumination configuration shown schematically in Fig. 1a. The output of a 20-W tungsten halogen lamp was focused by a 150-mm-focal-length lens while a 6-mm-diameter mirror was used to direct the focal point onto the end of the optical fiber. This end of the optical fiber was located at the focal point of the spectrometer. The distal end of the optical fiber served

Received 11 April 1988.
* Author to whom correspondence should be sent. Present address: Pacific Scientific, 2431 Linden Lane, Silver Spring, MD 20910.

0003-7028/88/4208-1549$2.00/0

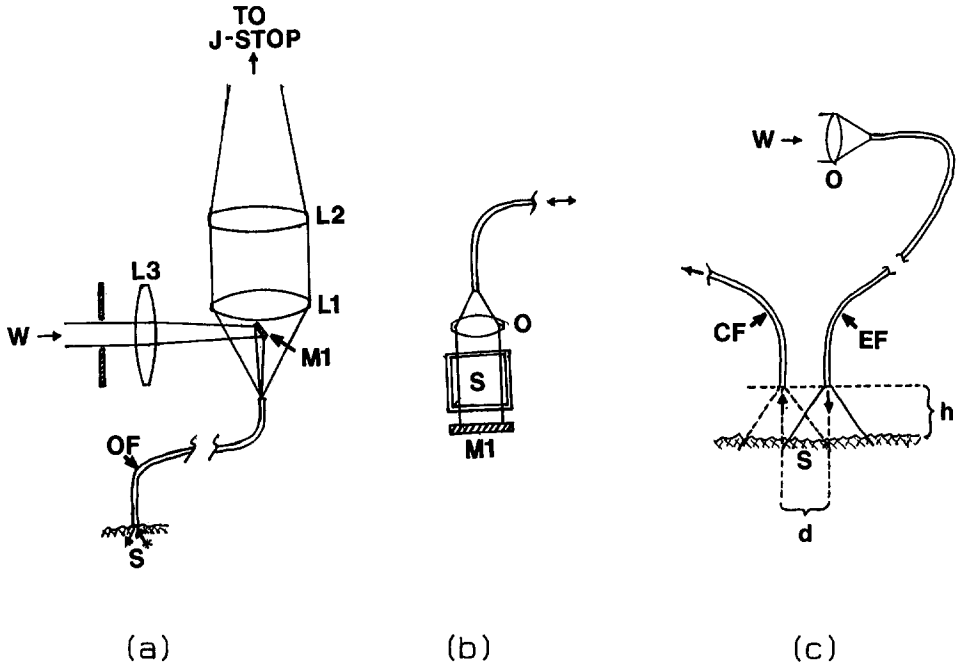

FIG. 1. Optical fiber sampling probes for reflectance and transmission measurements: (a) single-fiber reflectance probe: W, tungsten source; L3, 150-mm lens; M1, 6-mm mirror; OF, optical fiber; S, specimen; L1, collection lens; L2, NA matching lens; J-stop, Jacquinot stop of the spectrometer; (b) single-fiber transmission probe: O, collimating microscope objective; S, specimen; M1, flat mirror; (c) dual-fiber reflectance probe: W, tungsten source; O, focusing microscope objective; EF, excitation optical fiber; S, specimen; CF, collection optical fiber; *h*, height of probe above specimen; *d*, distance between EF and CF.

as a reflectance probe, which was placed on the surface of the specimen. Figure 1b shows the way that the probe tip was modified for transmission measurements. Light coming out of the fiber is collimated by a microscope objective, after which the light passes through the specimen and then a flat mirror reflects the light back through the specimen, where it is then coupled back into the fiber by the microscope objective.

The dual-fiber reflectance probe consisted of one 4.5-m length of optical fiber that sent light to the specimen (excitation fiber) and a second 1.5-m length which collected scattered light from the specimen (collection fiber) and sent it to the spectrometer. The coupling geometry between the collection fiber and the spectrometer was the same as that for the single-fiber probe, except that the back-illumination mirror was not used. Light from a 20-W tungsten halogen lamp was coupled into the excitation fiber with the use of a 0.40 NA microscope objective. When necessary, wire screens were used to reduce the intensity of light entering the fiber. The reflectance probe tip consisted of the bare fiber end faces in various orientations with respect to each other and the specimen. As shown in Fig. 1c, the excitation and collection fibers were parallel, with their end faces in the same plane. In the spectra shown in this paper, the height, *h*, above the specimen ranged between 0 and 20 mm while the distance, *d*, between the centers of the fibers ranged between 1.1 mm (fiber buffers in contact) and 3.6 mm. All spectra were measured with an *h* of 0 mm and *d* of 1.1 mm unless otherwise noted. For comparison, reflectance measurements of KCl and glycine were made with a conventional diffuse-reflectance FT-IR attachment, the Collector from Spectra-Tech.

Most of the spectra are displayed in pseudoabsorbance units. Reflectance power spectra were first converted to reflectance units as defined in Eq. 1. P_s indicates the power spectrum of the specimen, while P_r indicates the power spectrum of crystalline KCl collected with the same instrumental configuration and sampling conditions as the specimen. Pseudoabsorbance spectra were calculated with the use of Eq. 2.

$$R = P_s/P_r \quad (1)$$

$$A_r = -\log(R). \quad (2)$$

Crystalline reagent-grade KCl was obtained from J. T. Baker, Inc. (100.1% by Ag titration). Crystalline glycine (98%) was obtained from Aldrich Chemical Co. Filter paper was Whatman #5. Nitrobenzene was manufactured by Mallinckrodt (unknown purity).

RESULTS AND DISCUSSION

The optical attenuation of the fused-silica fiber ultimately limits the spectral range of our remote reflectance measurement. In Fig. 2a we see that the background reflectance power spectrum as measured with the InSb detector extends from 0.91 to 2.86 μm when the measurement is made with a diffuse-reflectance attachment. This background spectrum shows the broad and smooth shape of the blackbody emission from the tungsten lamp filament, with regions of sharp water-vapor absorptions (~2.75 and 1.85 μm). The background also shows the beginning of the long wavelength cutoff that is caused by the quartz beamsplitter and a glass optical filter used to reject visible light from the source. Figure 2b is a power spectrum of the optical fiber reflectance system which has a cutoff at 2.15 μm and also has many smaller absorption features. After performing the experiments pre-

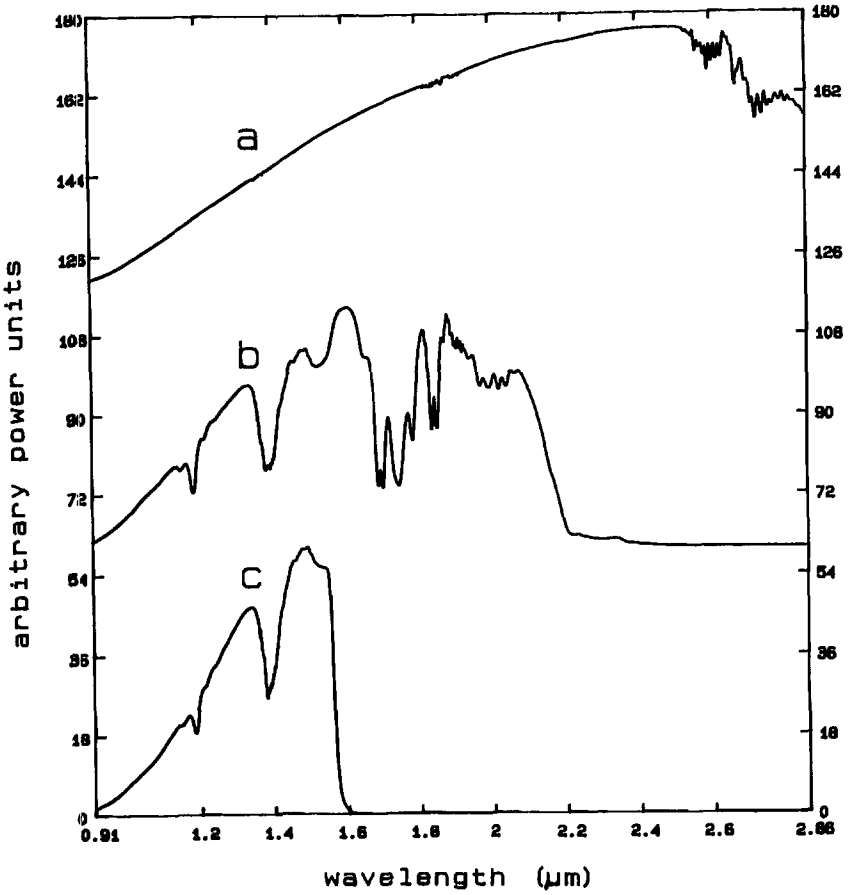

FIG. 2. KCl reflectance power spectra collected with varying detection and sampling arrangements of the FT spectrometer: (a) InSb detector and a Spectra-Tech diffuse reflectance cell; (b) InSb detector and an optical fiber reflectance system; (c) InGaAs detector and an optical fiber reflectance system. Spectra have been scaled and offset for this plot.

sented in this paper, we discovered that these absorption features are predominantly a result of light propagation in, and absorption by, a thin silicone coating between the glass cladding and the nylon buffer. This problem

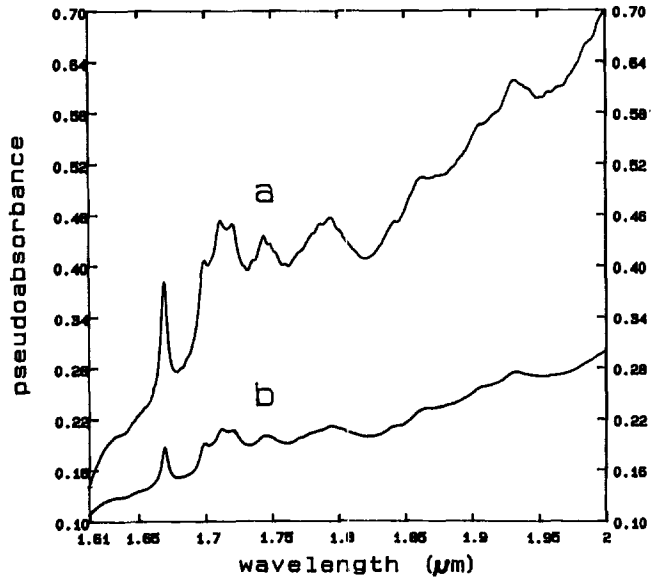

FIG. 3. A portion of the glycine pseudoabsorbance spectra collected with the InSb detector: (a) 3-min scan with the dual-fiber probe; (b) 1-min scan with the Spectra-Tech diffuse reflectance attachment. Spectral offsets are arbitrary.

can be alleviated by removal of cladding modes or by the use of fibers which have less of a tendency to propagate cladding modes. The background absorption at 1.4 μm is partly caused by the fused silica of the lenses. When the reflectance measurement is made with an InGaAs detector, the cutoff occurs at about 1.56 μm. This is seen in Fig. 2c.

Despite the discontinuities in the power spectra of the remote reflectance sensor, good pseudoabsorbance spectra can be obtained. Figure 3 shows a portion of the pseudoabsorbance spectrum of crystalline glycine as measured with the two-fiber reflectance system and the Spectra-Tech reflectance cell. The glycine absorbances are quite consistent. If the background spectrum of the fiber remains constant between sample and reference measurements, the excellent frequency precision of the FT spectrometer allows accurate ratios to be performed on the power spectra.

The phrase "excitation volume" will be used in this report to mean the particular region of the specimen with which the light from the excitation fiber interacts to a significant degree. The phrase "collection volume" indicates the region of the specimen from which the collection fiber could collect a significant portion of light if it were emitted from that region. This terminology is useful for explaining why different sampling configurations have different sample pathlengths and have varying specular reflection contributions. Figure 4 contains a

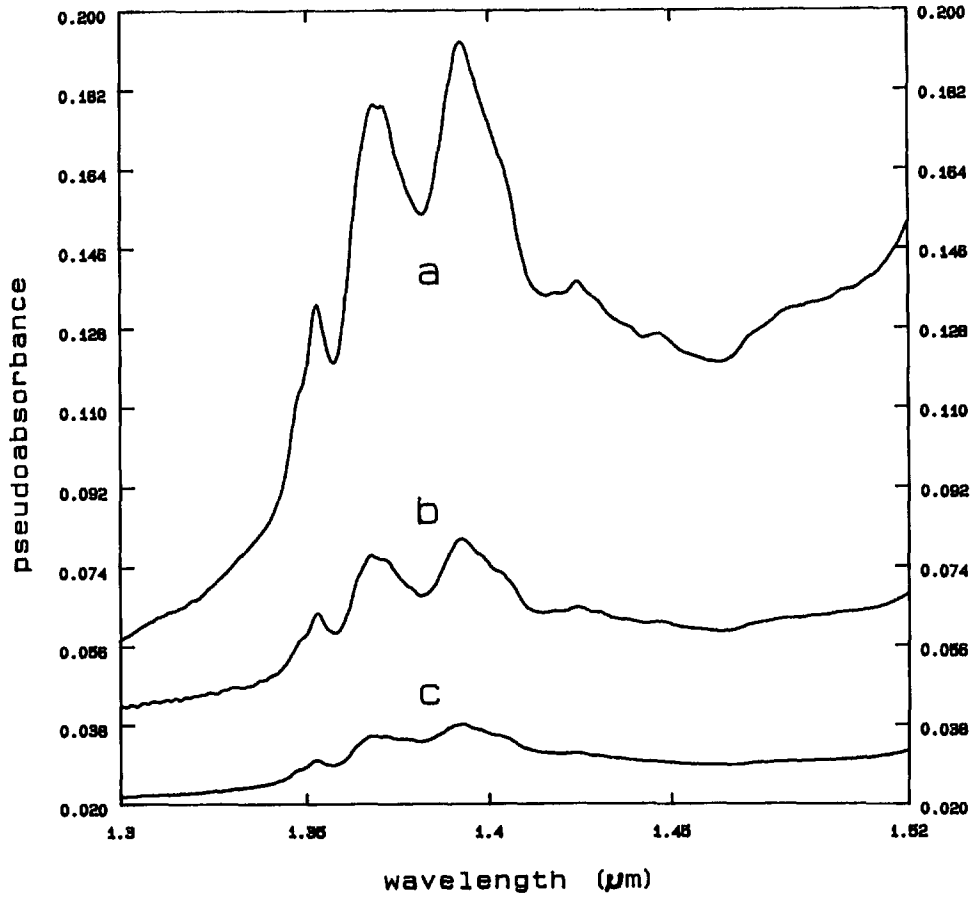

FIG. 4. A portion of the glycine pseudoabsorbance spectra collected with various sampling configurations: (a) 3-min scan of a dual-fiber reflectance measurement obtained with the InSb detector; (b) 1-min scan with the Spectra-Tech diffuse reflectance attachment and the InSb detector; (c) 2-min scan of the single fiber reflectance sensor with the InGaAs detector. Spectral offsets are arbitrary.

portion of the pseudoabsorbance spectra of crystalline glycine obtained with three different sampling configurations including the dual-fiber probe, the diffuse-reflectance attachment, and the single-fiber probe. The absorbance peaks for the single-fiber probe are smaller than those seen with either the dual-fiber probe or the conventional reflectance cell. This is partly the result of a shorter effective pathlength or, alternatively, a greater proportion of specularly reflected light. With the single-fiber probe, the excitation and collection volumes are identical, and the collection of a great deal of specularly reflected light is favored. Absorbance peaks are greater with the dual-fiber geometry because the excitation and collection volumes are offset, and this increases the effective pathlength that the light must travel in the specimen before being collected. As will be described later, control of this pathlength is a useful feature of the dual-fiber system. The conventional FT-IR diffuse reflectance measurement has absorbance peak magnitudes that are intermediate between those observed with the single- and dual-fiber probes. It appears that the effective pathlength of this attachment is intermediate between the single- and dual-fiber probes.

Specular reflection from the surface of the specimen is not the only source of noninteracting signal with the single-fiber reflectance probe. Specular reflections off both faces of the optical fiber also are measured by the spectrometer. Collection of reflected light from the crystalline glycine was about 1–3% of the incident light for the single fiber geometry, while the specular reflection from the end faces of the fiber is estimated to be about 8%. With such a large stray-light background, it was surprising that an absorbance signal was observable. The fact that the glycine absorbance peaks were not completely distorted by the large stray light signal is probably a result of the fact that glycine is a very weak absorber in this spectral region. The quality of single-fiber reflectance spectra would certainly be improved by probe designs with reduced stray-light intensity.

The single-fiber probe can also be configured for transmission measurements, as shown in Fig. 1b. Single-fiber transmission spectra of nitrobenzene are shown in the lower portion of Fig. 5. Stray light from end-face reflections is about 8% of the total intensity, and this reduces the apparent magnitude of the stronger absorptions. The stray light can be quantified by measuring the intensity when the light beam is prevented from being coupled into the fiber on the return to the spectrometer. This was accomplished by placing a strongly absorbing material at the sample position. Using this measurement to correct both sample and reference power spectra before calculation of the absorbance spectrum resulted in a slightly increased magnitude of the stronger absorbance peaks. This result is apparent upon comparing spectra b and c of Fig. 5. Even with the stray light correction, absorbance values greater than 2.5 would probably be

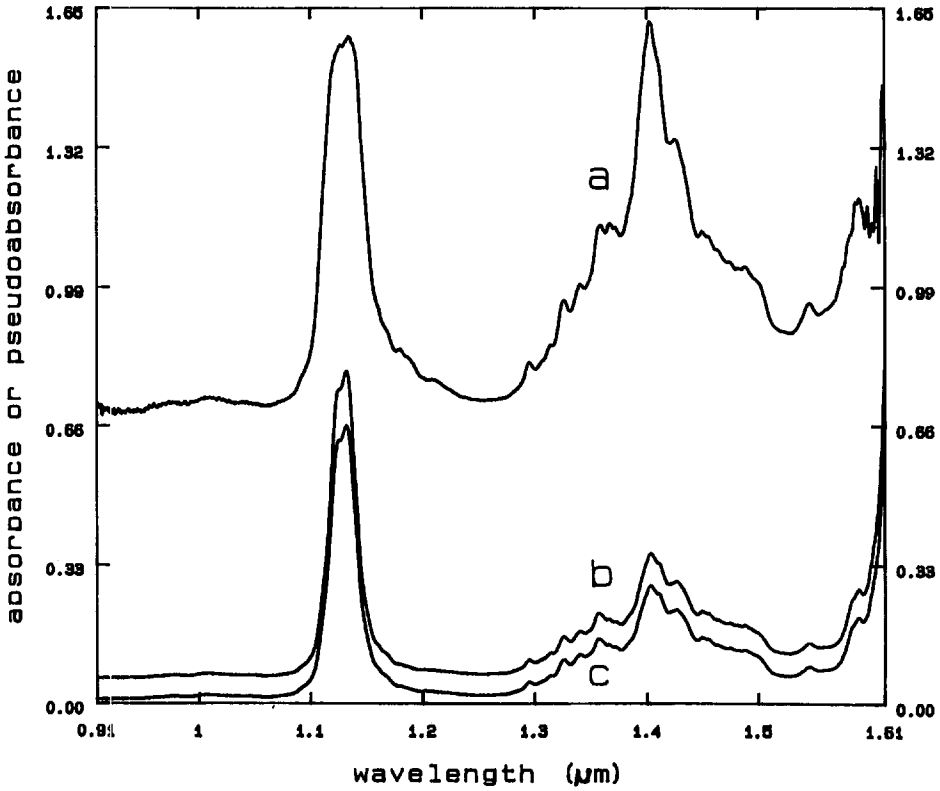

FIG. 5. Spectra of liquid nitrobenzene: (a) 1-min scan obtained with the dual-fiber reflectance probe; (b) and (c) 2-min scans obtained with the single-fiber absorbance probe with a 2.00-cm effective pathlength and where b has been corrected for stray light. Spectral offset is arbitrary in all cases.

nonlinear with concentration. If stray light intensity can be decreased, the usable absorbance range will be increased. However, stray light will always be more difficult to reduce in probes which use the same optical path to send and to collect sample light, when compared with similar systems in which different optical paths are used.

Dual-fiber reflectance measurements are more promising than single fiber measurements. The stray-light limitations of single-fiber measurements are not present. This allows the full dynamic range of the detection system to be used. Furthermore, the improved light throughput and the independence of the excitation and collection volumes make a number of probe configurations possible. These configurations were explored with the use of the InGaAs detection system because this detector was more sensitive than the InSb detection system. To some degree, the results obtained with the dual-fiber reflectance probe using the InGaAs detector system can be extended to a similar system using the InSb detection system. However, it is fortunate for near-IR absorption spectroscopists (but unfortunate for near-IR Raman spectroscopists) that the spectral region spanned by the very sensitive InGaAs detector (0.92–1.56 μm) has a reasonable amount of chemical absorption information.[7] A correlation table indicates that overtone and combination bands of OH, CH, and NH vibrations are present.[8] The many broad and narrow absorbances of the glycine spectra shown in this paper are characteristic of hydrogen-bonded crystal structures and are excellent candidates for quantitative and qualitative analysis.

With the maximum amount of light coupled into the excitation fiber, it was possible to obtain reflectance spectra from elastic scattering of organic liquids. This is an interesting measurement because the power spectrum recorded by the spectrometer is a function of both the scattering and absorption of the liquid. Weakly absorbed wavelengths have longer effective pathlengths than do strongly absorbed ones. This can be seen in the nitrobenzene spectra in Fig. 5a. Sharp absorbance bands appear broadened, and small absorbances are greater, when compared to the fixed-pathlength transmission measurement. This result is similar to absorbance measurements made in an etalon cavity, where the effective pathlengths are odd numbers of passes across the specimen cell.[9] However, with the reflectance system all pathlengths are possible, not just an integer multiple of a certain length. Dasgupta developed a helical multipath cell and showed that it could be used to extend the dynamic range of absorbance measurements.[10] Dynamic range extension might be a significant advantage for near-IR measurements because there is generally a large range of molar absorptivities for near-IR absorptions. This would be particularly true with single-beam FT measurements, because weakly absorbing regions often limit the dynamic range of the measurement of the entire spectrum.

It is difficult to obtain a background spectrum for reflectance measurements of liquids. CCl_4 was initially tried as a reference liquid because it has no near-IR absorption and has an index of refraction comparable to the specimen. Unfortunately, it is also a very weak scatterer, so that the effective pathlength was too great to be practical. As a result, scattering from dry granular KCl was used as the background. Consequently, the NA of the fiber

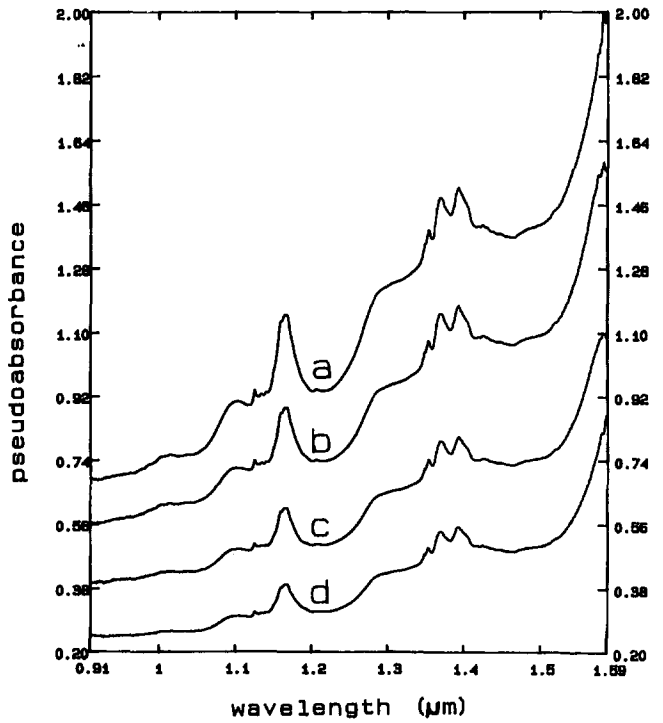

FIG. 6. Pseudoabsorbance spectra of crystalline glycine obtained with varying distances between the excitation and collection fibers where the probe rests on the surface of the specimen; separation was 3.6 mm for a, 2.9 mm for b, 1.7 mm for c, and 1.1 mm for d. Scans were 50 s for each spectrum. Spectral offset is arbitrary.

was significantly different for sample and reference spectra.

The back-scattering measurement of liquids is limited to strongly scattering liquids. To overcome this limitation, one might add additional components, such as an etalon cell or a strongly scattering surface, to the probe at the end of the optical fiber.

It was previously noted that the dual-fiber reflectance probe had a greater effective absorbance pathlength than is observed with the single-fiber probe. The pathlength can be further increased by increasing the distance, *d*, between the centers of the fibers. Figure 6 shows reflectance spectra of crystalline glycine taken with *d* ranging from 3.6 to 1.1 mm. The effective absorbance pathlength is about 3 times greater for *d* of 3.6 mm compared to *d* of 1.1 mm. As the two fibers in the reflectance probe are separated, the light throughput decreases quite dramatically, as can be seen in Fig. 7 for the reflectance of crystalline KCl. With this particular specimen, for *d* up to about 7 mm, one could compensate for the throughput loss by increasing the amount of light coupled into the excitation fiber. For the same nominal resolution and data acquisition time, the S/N obtained in measurements made at larger fiber separations would be limited by the maximum source intensity.

The dual-fiber probe was also used to obtain spectra without contacting the specimen surface. As the height, *h*, above the specimen was increased, the reflected power first increased and then decreased. This can be seen in Fig. 8. The increase in reflected power was caused by the better overlap between the excitation and collection volumes. As such, the maximum measured power occurred at greater *h* when *d* was increased. These effects are well

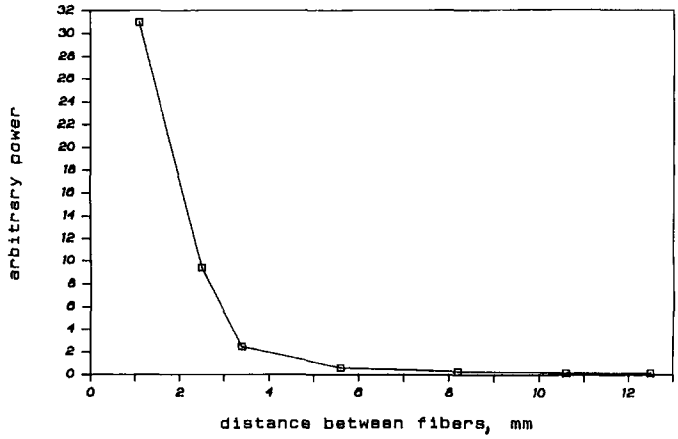

FIG. 7. Relative measured power from crystalline KCl obtained as a function of fiber separation within the dual-fiber probe where the probe rests on the surface of the specimen.

known and are used for noncontact displacement measurements.[11] Light throughput was sufficient to allow us to measure spectra up to a height of about 30 mm without reducing the amount of light striking the detector.

The effective absorption pathlength for above-surface measurements was enhanced when the excitation volume was separated from the collection volume. With *d* small, the glycine reflectance spectra show greater pathlength only very near to the surface, as is seen in Fig. 9a. Note that, above a height of 3 mm, essentially all the reflectance signal is obtained from the region where the excitation and collection volumes overlap, and this factor results in a constant observed pathlength. When the fibers are farther apart, increased pathlength is observed at greater height above the specimen, as is seen in Fig. 9b.

Separation of the excitation and collection volumes can be used for depth discrimination of a multilayered specimen. To simulate a depth dependent application, we analyzed a specimen that consisted of a 0.23-mm-thick piece of filter paper over a relatively thick layer of crystalline glycine. Spectra of the paper over KCl, pure glycine, and the bilayered sample can be seen respectively in a, c, and e of Fig. 10. Features of the glycine

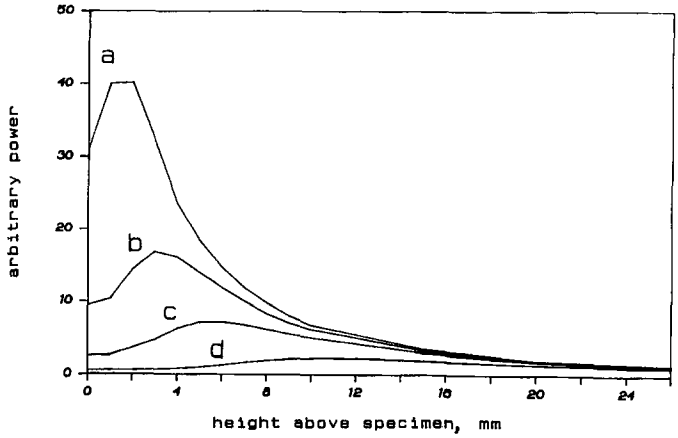

FIG. 8. Relative power measured with the dual-fiber reflectance probe over a flat crystalline KCl surface as a function of height above the surface. Fiber separations within the probe are 1.1 mm for a, 2.5 mm for b, 3.4 mm for c, and 5.6 mm for d.

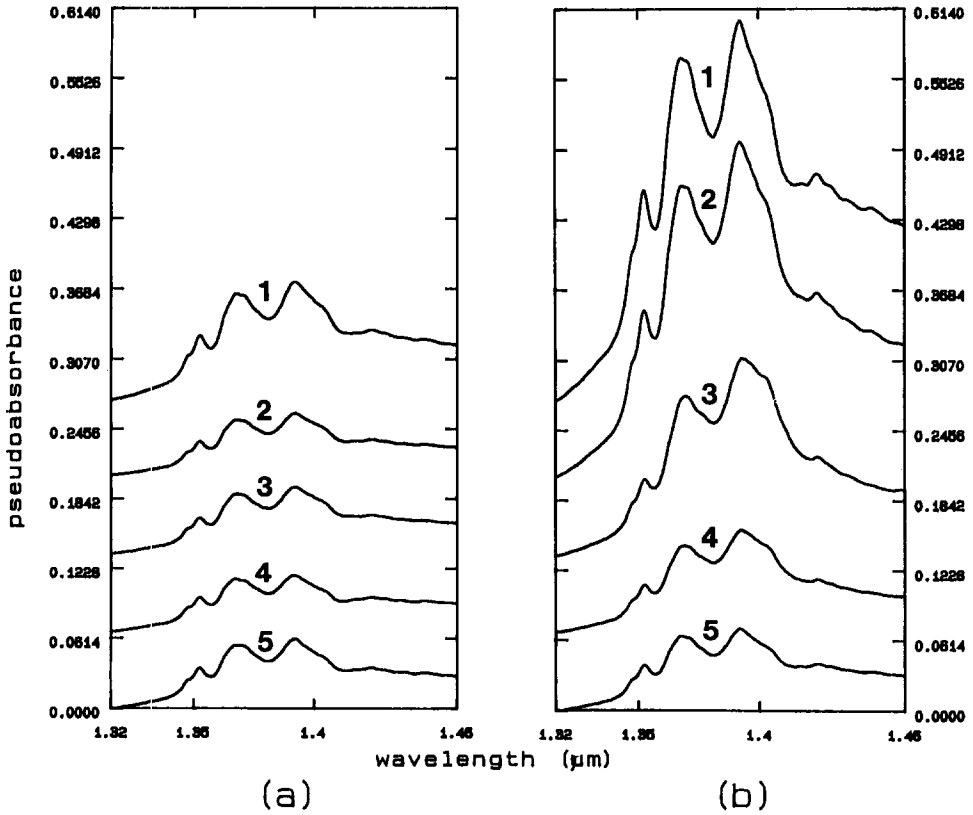

FIG. 9. A portion of the crystalline glycine pseudoabsorbance spectra measured with the dual-fiber probe at various heights above the flat surface of the specimen and for two different separations between the excitation and collection fibers. In a the probe fibers are 1.1 mm apart, while in b the fibers are 3.6 mm apart. The height of the probe above the specimen is 0 mm for the spectra labeled 1, 3 mm for 2, 6 mm for 3, 10 mm for 4, and 20 mm for 5. Spectral offset is arbitrary.

spectrum are readily observed in the bilayer specimen. With the use of the pure spectra, it is a simple matter to separate the signal from each component by eye while using the interactive spectral-subtraction software supplied with the FT-IR. As seen in b and d of Fig. 10, this method works well, except at wavelengths where both components absorb strongly. The excellent light penetration was apparent from the fact that the magnitude of the glycine absorbance signal was only reduced to about half that of the magnitude of absorption of the pure glycine specimen. When the probe fibers were separated, the absorbance pathlength for both the paper and the glycine increased. However, the glycine pathlength increased to a greater degree. This can be seen in Fig. 11.

To quantify the enhancement of the subsurface absorbance relative to the surface layer absorbance, we made a least-squares curve fit of the paper-over-KCl spectrum and the pure glycine spectrum to the bilayer spectra. Table I shows the ratios of the regression coefficients for paper absorption to glycine absorption. It is not strictly correct to obtain absolute coefficients in this manner, because the pathlength of the glycine depends on the height above the specimen (which differs by the thickness of paper when one is comparing the mixture and pure spectra), and the pathlength in the paper depends on the reflectance of the material underneath the paper (KCl or glycine). However, the ratios of the regression coefficients show semiquantitatively how the fiber tip separation can be used to distinguish the two layers. With d of 1.1 mm, the mixture spectrum is mostly paper, while when d is 3.6 mm, the mixture spectrum is mostly glycine. The result here has obvious application to situations where one wants to sample a substance through a thin packaging material or surface layer. Furthermore, depth profiling is possible because, as the probe fibers are separated, the absorbance features of the underlying material increase more rapidly than do those of the material closer to the surface. Pattern recognition techniques ought to be able to deduce some degree of depth profile from reflectance data obtained as a function of fiber separation. Multiple fiber geometries could be employed to increase illumination intensity, thus allowing depth profiling of a variety of samples in a wider spectral region. Imaging of an underlayer based on the near-IR spectral differences of the layers has been shown to be a viable technique.[12] The spatial depth discrimination technique reported here provides an alternative means of near-IR depth imaging.

In FT spectrometry, the user can easily change the nominal resolution of the spectrum measured. High-resolution remote reflectance spectra can be obtained in a reasonable period of time because of the high irradiance of the source and the multiplex advantage. With the remote reflectance system, interferometer throughput was low enough to allow better than 0.5-cm^{-1} nominal resolution. Figure 12 shows the 2-cm^{-1} resolution spectrum of a small portion of the glycine spectrum compared with the 8-cm^{-1} resolution that was chosen for most of the measurements in this paper. The S/N of the low-resolution spectra should be nearly double that of the high-resolution scan, which was signal averaged for 6 times as

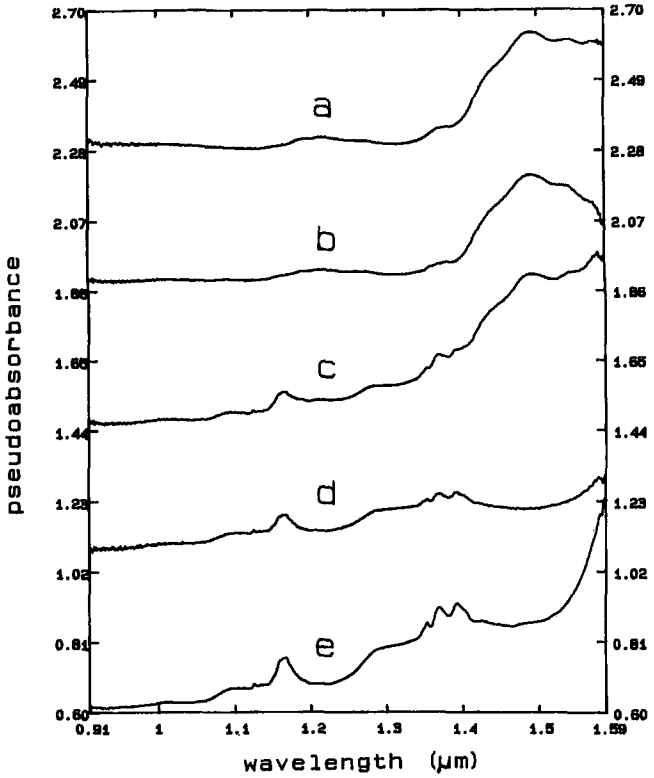

FIG. 10. Dual-fiber pseudoabsorbance spectra of 0.23-mm-thick filter paper and crystalline glycine each collected with a 50-s scan time: (a) spectrum of a layer of the paper over KCl; (b) spectrum resulting from subtraction of e from c; (c) spectrum of a layer of the paper over glycine; (d) spectrum resulting from subtraction of a from c; (e) spectrum of glycine.

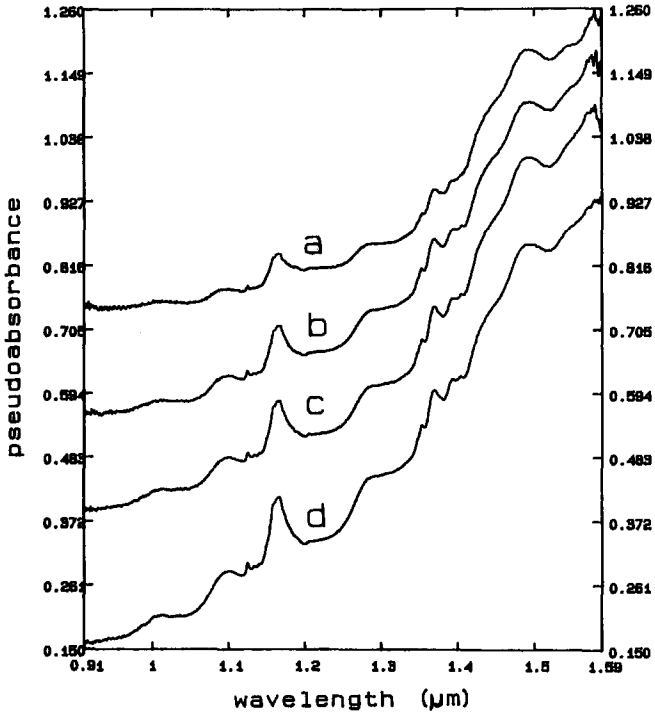

FIG. 11. Dual-fiber pseudoabsorbance spectra of 0.23-mm-thick filter paper over crystalline glycine at varying distances between the excitation and collection fibers: (a) 1.1 mm; (b) 1.7 mm; (c) 2.9 mm; and (d) 3.6 mm. Scan time was 50 s and spectral offset is arbitrary.

long. The glycine absorptions appear sharper in the higher resolution scan, despite greater noise amplitude. Resolution of 8 cm^{-1} is high resolution when compared to a standard near-IR spectrometer configuration (resolution near 1 μm is 0.8 nm compared with 10 nm for a Technicon InfraAlyzer 500). With the resolution reduced by half, the collection time to obtain the same S/N would theoretically be reduced by a factor of 4. If the nominal resolution were set to 100 cm^{-1} (10 nm at 1 μm) at the same optical throughput, only 0.32 s would be needed to obtain the same S/N as obtained by a 50-s, 8-cm^{-1} scan. For a nominal resolution of 25 cm^{-1} (10 nm at 2 μm), 5.2 s would be required. This time savings could be used to signal average, so that one might effectively employ the less sensitive InSb detector, which can measure over the entire near-IR window of fused-silica optical fibers.

Performing spectroscopy over optical fibers was straightforward, but not completely without complication. Periodically, spectral anomalies were observed as small negative or positive peaks where fiber absorptions were known to occur. A major cause of this anomaly was found to be the difference in the angles of light propagation in the waveguide between sample and reference measurements. Relatively strong spectral anomalies could be induced by changing the NA of light entering or exiting either the excitation or collection fibers between reference and sample measurements. This has two spectral effects; the major one is that the effective pathlength through the fiber is changed, and a minor effect results from the variation in energy distribution between the core and cladding materials which have different absorptions. Sample particle size or overlap of the excitation and collection volumes also can affect the angle of light propagation in the collection fiber. With the samples and geometries employed in this study, the effect of these factors was relatively minor. Height of the probe above the surface of the specimen was not found to produce spectral anomalies unless the overlap of the excitation and collection volumes was significantly altered. Spectral anomalies resulting from waveguide absorption could likely be minimized by appropriately placed mode scrambling or stripping devices and/or by reducing the NA of light collection from the optical fiber. Neither possibility was explored in depth.

The optical efficiency of the fiber spectrometer system deserves comment. Without considering source intensity or source coupling efficiency of the system employed in the measurements described in this report, optical throughput is limited by the diameter and NA of the collection fiber. The throughput of the detection system is designed to be slightly greater than this, so that the detector is evenly illuminated. If, instead, a 2.0 sr detection optic had been used, the 600-μm source image

TABLE I. Ratio of the regression coefficients of glycine and paper, R_g/R_p, calculated by least-squares curve fitting of the pure spectra to the mixture spectra which were obtained with the dual-fiber reflectance probe as a function of the distance, d, between the fibers of the probe.

d, mm	R_g/R_p
1.1	0.60
1.7	0.92
2.9	0.97
3.6	1.39

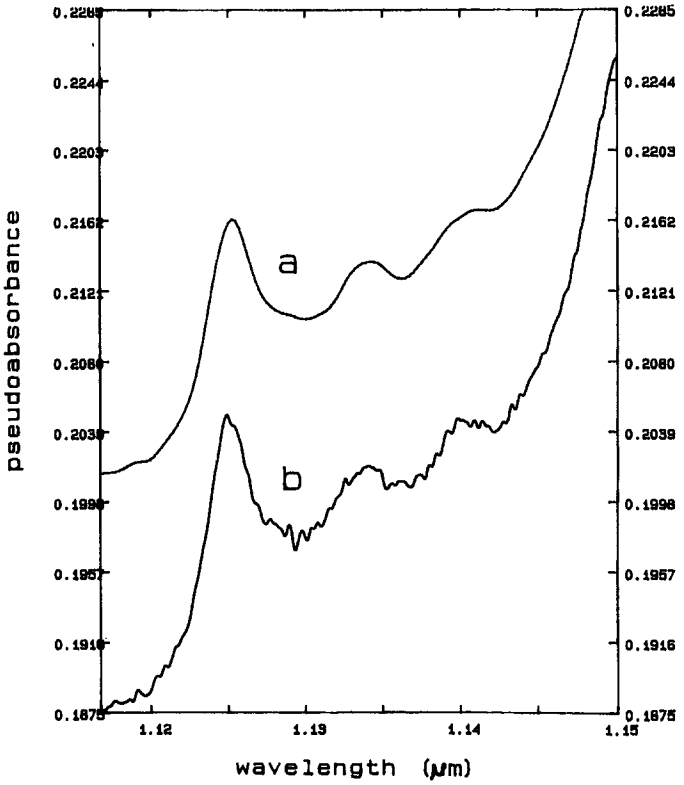

FIG. 12. A portion of the pseudoabsorbance spectra of crystalline glycine collected with different instrumental resolution: (a) 50-s scan at 8-cm^{-1} resolution; (b) 6-min scan at 2-cm^{-1} resolution. Spectral offset is arbitrary.

could be reduced from 1-mm to 189-μm diameter. Thermal noise in the detector should decrease as the square root of the detector area so that if the detector is not saturated by the increased power density, amplifier noise does not dominate, and if all other factors are the same, S/N should improve by a factor of 5.3.

All else held constant, signal is proportional to the area of the fiber end face, and noise is proportional to the square root of the detector area. Given a certain detector-optic/source-optic combination, the area of the image of the source at the detector is proportional to the area of the source. Thus S/N varies with the square root of the source diameter. With a 100-μm optical fiber of the same NA as the 600-μm fiber, we could have employed a 32-μm-diameter detector and achieved about 0.41 the S/N of a system optimized for a 600-μm-diameter fiber. This would be a factor of 2.2 better than the system used in this paper.

The optical system is reversible, so that the detector plus its associated optics can be exchanged for the source plus its associated optics, with no loss in efficiency. This capability allows modulation of the light before interaction with the specimen. In the presence of stray light, premodulation of the light would improve the measurement. It would also allow a single interferometer to be used to modulate light for a large number of probe fibers. With a suitable source configuration, if operated near 1.0 μm at 8-cm^{-1} resolution, the 3.0-cm-diameter mirrors of our Michelson interferometer are capable of filling the aperture of a 4.5-mm-diameter bundle of fibers each with an NA of 0.25. If only 32-cm^{-1} resolution (3.2 nm at 1 μm) is desired, the interferometer can fill a 9.1-mm-diameter bundle. Each fiber of the bundle could be used for a separate transmission or reflectance experiment and have its own detection system. It would be simple to digitize the signal from one probe and then another, but simultaneous measurements would be desirable for some applications, such as a multiple tip probe for spatially resolved reflectance measurements. The A/D converter in the Perkin-Elmer 1800 can digitize data at a rate of over 94 kHz. If the interferometer moving mirror velocity is set at 0.05 cm/s, and nominal resolution is 32 cm^{-1}, each data collection scan will take 0.31 s. This is a data collection rate of 3.16 kHz. If one can electronically switch between different preamplifiers and accurately offset digitization between zero crossings of the reference laser, up to 30 detector responses could be recorded in a single scan. Every 30th data point would then be combined into sets that form an interferogram for each probe, and the spectrum calculated for each. Variations in mirror velocity might prevent accurate offset of digitization.

Collection of near-IR reflectance signals by a single optical fiber opens definite possibilities for a simple remote probe capable of spatially resolved measurements. A fiber bundle probe would consist of an array of intermixed illumination and collection fibers where each collection fiber is a separate measurement channel. The degree of spatial resolution that one would achieve would depend on the diameter and NA (and perhaps microoptics) of the excitation and collection fibers as well as the scattering characteristics of the specimen. Depth discrimination for a single channel could also be done with the same probe simply by illumination of the specimen with fibers that are a fixed radial distance from the collection fiber followed by measurements at varying radial distances from the collection fiber.

CONCLUSIONS

Near-IR reflectance spectroscopy over a single optical fiber or a pair of optical fibers was performed with the use of a modified FT-IR spectrometer. A dual-fiber probe was found to be quite versatile. The dual-fiber sensor could be designed to increase the effective pathlength through the specimen and was useful for reflectance spectroscopy without physical contact between the probe and specimen. Light throughput and detector sensitivity were good enough to allow reflectance spectroscopy of scattering organic liquids. Reflectance spectroscopy of liquids can be used to reduce dynamic range requirements for multiplex near-IR spectroscopy.

Separation of the excitation and collection fibers was shown to be useful for discriminating different depths in a specimen. With the use of pattern recognition algorithms, this spatial resolution technique might be useful for depth profiling of various layers in a specimen. Some degree of spatial resolution across the surface of a specimen would also be possible with the use of multiple collection fiber channels. When combined with the inherent spectral imaging capability of near-IR reflectance spectroscopy, the aforementioned spatial resolution techniques provide a potentially very useful new tool for remote sensing and imaging of specimens.

ACKNOWLEDGMENTS

We would like to thank the National Science Foundation for financial support of this research, and Perkin-Elmer corporation for donation of the FT-IR that was used in this study.

1. E. Stark, K. Luchter, and M. Margoshes, Appl. Spectrosc. Rev. **22**, 335 (1986).
2. D. E. Honigs, Anal. Instrument. **14**, 1 (1985).
3. L. G. Weyer, Appl. Spectrosc. Rev. **21**, 1 (1985).
4. D. D. Archibald, L. T. Lin, and D. E. Honigs, Appl. Spectrosc. **42**, 468 (1988).
5. W. F. X. Frank, W. Goertz, and H. H. Belz, Appl. Spectrosc. **41**, 323 (1987).
6. P. M. Fredericks, P. J. Samson, and A. D. Stuart, Appl. Spectrosc. **41**, 327 (1987).
7. B. Tenge and B. R. Buchanan, Appl. Spectrosc. **41**, 779 (1987).
8. R. F. Goddu and D. A. Delker, Anal. Chem. **32**, 140 (1960).
9. P. K. Dasgupta and J. S. Rhee, Anal. Chem. **59**, 783 (1987).
10. P. K. Dasgupta, Anal Chem. **56**, 1401 (1984).
11. L. J. Lagace and C. D. Kissinger, "Non-Contact Displacement and Vibration Measurement Employing Fiber Optic and Capacitance Transducers," in *Proceedings of the 23rd International Instrumentation Symposium*, B. Washburn, Ed. (Instrument Society of America, Research Triangle Park, North Carolina, 1977), pp. 1–10.
12. R. A. Lodder and G. M. Heiftje, Appl. Spectrosc. **42**, 313 (1988).

Raman Spectroscopy over Optical Fibers with the Use of a Near-IR FT Spectrometer

D. D. ARCHIBALD, L. T. LIN, and D. E. HONIGS*

Department of Chemistry, University of Washington, Seattle, Washington 98195

A commercial Fourier transform infrared (FT-IR) spectrometer was modified for remote near-IR Raman spectroscopy. In one configuration, a single optical fiber was used to guide the excitation light to the specimen and to collect scattered light from the specimen. In an alternative configuration, separate fibers were used for excitation and collection. The optical fiber probes were used to record the Raman spectra of both liquid and solid specimens. The Raman scattering of the optical fibers interfered with the analyte signal. This fiber interference was affected by the optical properties of the specimen and the optical sampling configuration. These interferences were partially removed by subtracting a background spectrum. Potential applications and improvements are discussed.

Index Headings: **Spectroscopy (near-IR, remote, Raman, FT-IR); Optical fiber.**

INTRODUCTION

Optical fibers have been employed by Raman spectroscopists for coherent anti-Stokes Raman[1] and surface-enhanced Raman,[2] as well as resonance and normal Raman scattering, experiments.[3] Raman sampling configurations that incorporate optical fibers have been designed for remote monitoring,[4–8] efficient collection,[9,10] uniform sample illumination,[11,12] pathlength enhancement for liquids,[13–15] and angular resolution of measurements.[2]

Much of the emphasis of optical fiber Raman sampling has come from the need for remote measurements with little sample preparation and relaxed optical tolerances. Unfortunately, because a remote probe is often intended for direct sampling of a process stream or environmental specimen, the likelihood of the presence of fluorescent impurities is greater than it is with a purified laboratory specimen. Where fluorescent impurities exist, they would totally dominate the remote Raman measurement unless the Raman were enhanced above the background. One way to circumvent the fluorescence problem is to employ near-IR excitation.

The feasibility of near-IR Raman has been demonstrated.[16] Unfortunately, near-IR Raman is a rather insensitive technique and is not suitable for trace analyses. However, normal Raman spectra are rich in analytical information about molecular connectivity of organic compounds and may be suitable for quantitation of minor components (>1%) of complex mixtures. Remote analytical near-IR Raman might be useful for the analyses for hydrocarbon or polymer processing. In these applications, the presence of luminescent impurities is likely, so that near-IR excitation would be a distinct advantage over visible excitation. Mid-IR absorption, of course, is an alternative vibrational spectroscopy that is many times more sensitive than normal Raman scattering for certain functional groups. However, unlike Raman scattering, mid-IR absorption is not sensitive to single and multiple carbon-carbon bonds in nonpolar environments. This is one reason why Raman spectroscopy is so often employed for the analysis of polymers. A further difficulty with mid-IR absorption is the fact that optical waveguides for this spectral region are inefficient and expensive.

The suitability of an FT-IR spectrometer for remote spectroscopy performed over a single optical fiber was described in an earlier paper.[17] It has also been reported that an FT spectrometer is suitable for measurement of near-IR light transmitted through a single optical fiber,[18,19] and this application was shown to be useful for remote near-IR transmission and reflectance measurements.[17,20] In this paper we describe the application of a sensitive near-IR FT spectrometer to measurement of Raman scattering collected by single optical fibers.

EXPERIMENTAL

Figure 1 shows the optical layout of the Perkin-Elmer Model 1800 FT-IR that was modified for the near-IR

Received 10 May 1988.
* Author to whom correspondence should be sent. Present address: Pacific Scientific, 2431 Linden Lane, Silver Spring, MD 20910.

0003-7028/88/4208-1558$2.00/0